

Linear and Cyclic Clusters of Hydrogen Cyanide and Cyanoacetylene: A Comparative *ab Initio* and Density Functional Study on Cooperative Hydrogen Bonding

Alfred Karpfen

*Institut für Theoretische Chemie und Strahlenchemie der Universität Wien,
A-1090 Wien, Währingerstrasse 17, Austria*

Received: February 27, 1996; In Final Form: May 3, 1996[®]

The equilibrium structures, the stabilization energies, the harmonic vibrational spectra, and the infrared intensities of linear and cyclic hydrogen cyanide, $(\text{HCN})_n$, and cyanoacetylene oligomers, $(\text{HC}_3\text{N})_n$, were calculated at the *ab initio* self-consistent field and at the Møller–Plesset second-order level, as well as with the aid of a density functional method. Several extended basis sets were applied. The systematic modifications of the most important properties characteristic for the C–H...N hydrogen bond in these two series of intermolecular clusters, in particular, the intermolecular distances, $R(\text{H} \cdots \text{N})$, the intramolecular distances, $R(\text{C}–\text{H})$, the interaction energies per hydrogen bond, with and without zero-point energy corrections, the C–H stretching frequencies, $\nu(\text{C}–\text{H})$, and their corresponding infrared intensities were monitored as a function of the oligomer size and are discussed in detail. The mode of convergence to the infinite chain limit is described and found to be qualitatively quite similar in both systems. From a quantitative point of view, all features usually attributed to hydrogen-bond nonadditivity are somewhat weaker for the cyanoacetylene clusters, mainly a consequence of the molecular size. Tentative assignments are suggested for the infrared active vibrations of larger cyclic cyanoacetylene clusters.

Introduction

The structures and the vibrational spectra of small, hydrogen-bonded clusters of hydrogen cyanide in the gas phase have been the subject of quite extensive investigations in the past decade.^{1–9} In addition to these microwave and high-resolution infrared gas phase experiments, thorough low-temperature matrix-spectroscopic studies of the infrared spectra of hydrogen cyanide clusters were carried out as well.^{10–16} Whereas the hydrogen cyanide dimer has definitely a fully linear equilibrium structure, the hydrogen cyanide trimer turned out to be of particular interest, since in this case the existence of two structurally distinctly different isomers in the gas phase, a linear and a cyclic form, could be proven.^{4,7} In the solid state, the hydrogen cyanide molecules arrange in extended, perfectly linear chains.¹⁷ The detailed description of the transition from the monomer to the molecular crystal and the understanding of the various factors governing the convergence behavior from the structural and spectroscopic properties of isolated, small linear, or cyclic vapor-phase clusters to those of the parallel chains in the HCN solid are the main motivations for these systematic experimental investigations.

Parallel to the just-mentioned experimental efforts, numerous quantum chemical investigations have so far been performed on the trimeric and larger complexes of hydrogen cyanide.^{3,16,18–25} From these theoretical calculations, the preferential stability of the fully linear ($\text{C}_{\infty\text{v}}$) aggregates and of the cyclic ($\text{C}_{3\text{h}}$) structures emerged in good agreement with the experimental findings. Theoretical investigations on infinitely extended, linear hydrogen cyanide polymers^{25–27} have also already been reported.

Hydrogen cyanide is, however, not the only molecule which can form *ideal linear* hydrogen-bonded chains in the solid state. A further interesting example is the very anisotropic crystal of cyanoacetylene, $\text{H}–\text{C}\equiv\text{C}–\text{C}\equiv\text{N}$, which also consists of extended linear, hydrogen-bonded chains.²⁸ In contrast to the large body

of experimental and theoretical investigations that has been devoted to the case of hydrogen cyanide, only comparatively few spectroscopic investigations have so far been reported on the cyanoacetylene dimer and on even larger cyanoacetylene clusters. The high-resolution infrared spectrum of the cyanoacetylene dimer in the gas phase was studied by Kerstel et al.²⁹ The first report of the vibrational spectra of larger cyanoacetylene clusters in the gas phase was provided very recently by Yang et al.³⁰

The structure^{31,32} and the vibrational spectra^{33–36} of the cyanoacetylene monomer are well-known. Similarly, the vibrational spectra of cyanoacetylene in the solid were quite thoroughly investigated.^{34,37,38} However, apart from several more accurate investigations of the cyanoacetylene monomer,^{32,39–41} only a few *ab initio* geometry optimizations of the linear cyanoacetylene dimer performed at the self-consistent field (SCF) level are available from the theoretical side.^{42,43} To the best knowledge of the author, *ab initio* calculations on the vibrational spectrum of the cyanoacetylene dimer have not yet been reported, nor are there any theoretical studies available in the literature that deal with the structure and the vibrational spectra of larger cyanoacetylene clusters.

In this work, we report the results of extensive, systematic *ab initio* calculations on the series of linear and cyclic hydrogen cyanide clusters, $(\text{HCN})_n$, and analogously, for the series of linear and cyclic cyanoacetylene clusters, $(\text{HC}_3\text{N})_n$. The reinvestigation of the hydrogen cyanide clusters will provide a basis for a detailed comparison with the hitherto less-well-known cyanoacetylene clusters. We aim at a consistent description of the equilibrium structures of these species and of their relative stabilities. Moreover, we also present the computed harmonic vibrational spectra in the C–H stretching region and the corresponding infrared intensities, i.e., we deal preferentially with the properties most relevant for the characterization of the C–H...N hydrogen bond in these clusters. In particular, we wish to provide an independent and sufficiently accurate

[®] Abstract published in *Advance ACS Abstracts*, June 15, 1996.

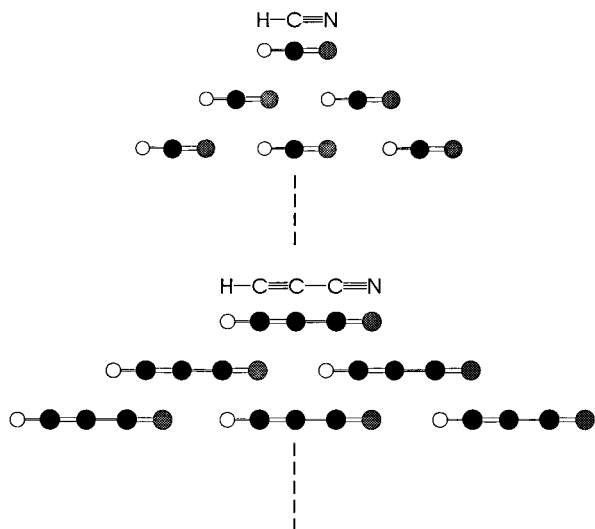


Figure 1. Schematic representation of linear hydrogen cyanide and cyanoacetylene clusters.

TABLE 1: Computed Equilibrium Structures of the Hydrogen Cyanide Monomer (All Values in Angstroms)

method	basis set	$r(\text{H}-\text{C})$	$r(\text{C}\equiv\text{N})$
SCF	I	1.0592	1.1328
	II	1.0588	1.1242
	III	1.0575	1.1253
B3LYP	I	1.0691	1.1572
	II	1.0673	1.1468
	III	1.0666	1.1472
MP2	I	1.0653	1.1778
	II	1.0647	1.1655
	III	1.0666	1.1686
CPF ^a	II	1.0660	1.1540
CPF ^a	III	1.0683	1.1568
ACPF ^b	II	1.0689	1.1600
CEPA ^c		1.0665	1.1534
experiment ^d		1.0655	1.1532

^a Reference 19. ^b Reference 22. ^c Reference 54. ^d Reference 55.

theoretical evaluation of the vibrational spectra which allows for the confirmation of the vibrational assignments of the new gas-phase infrared spectra of the cyanoacetylene clusters suggested by Yang et al.³⁰ and eventually serves as a guide in the assignment of yet-unassigned spectral features. Toward this end, we monitor the trends taking place upon increasing the cluster size and discuss the similarities in the aggregation behavior between these two molecules. The quantum chemical calculations were performed at various different levels of sophistication in order to be able to assess the methodical errors unavoidably present in the calculations of such large clusters.

Method of Calculation

All quantum chemical calculations performed in this work were done with the Gaussian 94⁴⁴ programs. The geometry optimizations and the calculations of the vibrational spectra were not only performed at the SCF level, but, as far the computational resources permitted, also within the framework of the Møller–Plesset second-order (MP2) perturbation theory,⁴⁵ and with the aid of one of the recently developed density functional approaches, the B3LYP method^{46–49} (Beckes 3-parameter exchange functional using the Lee–Yang–Parr correlation functional as implemented in Gaussian 94).

At each of these theoretical levels, three extended polarized basis were used. Basis set I is the 6-31G(d,p) basis.^{50,51} Basis set II is the 10s6p/6s Huzinaga^{52,53} basis set contracted to 6s4p/4s and augmented by a set of d functions on nitrogen and on

TABLE 2: Computed Equilibrium Structures of the Cyanoacetylene Monomer (All Values in Angstroms)

method	basis set	$r(\text{H}-\text{C})$	$r(\text{C}\equiv\text{C})$	$r(\text{C}-\text{C})$	$r(\text{C}\equiv\text{N})$
SCF	I	1.0581	1.1852	1.3915	1.1363
	II	1.0566	1.1788	1.3869	1.1276
	III	1.0559	1.1784	1.3885	1.1286
B3LYP	I	1.0667	1.2099	1.3726	1.1663
	II	1.0640	1.2005	1.3686	1.1557
	III	1.0635	1.2007	1.3692	1.1563
MP2	I	1.0640	1.2236	1.3770	1.1875
	II	1.0629	1.2116	1.3701	1.1752
	III	1.0652	1.2159	1.3728	1.1789
CEPA ^a		1.0624	1.2058	1.3764	1.1605

^a Reference 32.

TABLE 3: Computed Equilibrium Structures of the Hydrogen Cyanide Dimer (All Values in Angstroms)

method	basis set	$r(\text{H}-\text{C})$	$r(\text{C}\equiv\text{N})$	$r(\text{N} \cdots \text{H})$	$r(\text{H}-\text{C})$	$r(\text{C}\equiv\text{N})$
SCF	I	1.0598	1.1315	2.2996	1.0639	1.1335
	II	1.0595	1.1232	2.3276	1.0637	1.125
	III	1.0584	1.1242	2.3421	1.0622	1.1262
B3LYP	I	1.0698	1.1550	2.1743	1.0765	1.1577
	II	1.0681	1.1453	2.2250	1.0747	1.1474
	III	1.0672	1.1456	2.2312	1.0735	1.1479
MP2	I	1.0655	1.1758	2.2203	1.0706	1.1779
	II	1.0653	1.1641	2.2598	1.0706	1.1658
	III	1.0673	1.1670	2.2342	1.0729	1.1692
CPF ^a	II	1.0665	1.1526	2.2929	1.0709	1.1543
ACPF ^b	II	1.0694	1.1585	2.2608	1.0737	1.1603
experiment ^c				2.22		

^a Reference 19. ^b Reference 22. ^c Reference 56.

carbon, and a set of p functions on hydrogen. Basis set III is the 11s7p/6s Huzinaga^{52,53} basis set contracted to 7s5p/4s and augmented by two sets of d functions on nitrogen and carbon and a set of p functions on hydrogen. Basis sets II and III of this work are identical with the basis sets I and II used successfully in our previous calculations on HCN clusters (see Table 1 of ref 19). The use of still larger basis sets is computationally prohibitive for the problem in question.

All the theoretical information on the vibrational frequencies and intensities was obtained within the framework of the double harmonic approximation. In the presentation of the theoretical vibrational frequencies, we intentionally avoided scaling either the force constants or the frequencies in order to correct for methodical shortcomings (limited basis set, electron correlation approach) and simultaneously for anharmonic contributions. Rather, we prefer to discuss the vibrational spectra of the clusters in terms of the shifts with respect to the intramolecular vibrational frequencies of the monomers as computed at the various levels of sophistication. Furthermore, only the C–H stretching frequency region will be discussed explicitly.

Optimized Structures

The Monomers. The structures of the linear hydrogen cyanide and cyanoacetylene clusters treated in this work are sketched in Figure 1. The optimized equilibrium geometries of the hydrogen cyanide molecule as obtained with basis sets I–III at the SCF, B3LYP, and MP2 levels are compiled in Table 1 and compared with literature data. Analogous data for the cyanoacetylene molecule are collected in Table 2.

The main systematic failure appearing in the SCF-optimized structures, i.e., the consistently too short triple-bond lengths, is found for all three basis sets. The internal comparison between the computed MP2 and B3LYP equilibrium geometries reveals that for each of the three basis sets applied, the H–C and C–C single bond lengths agree satisfactorily, while in case of the

TABLE 4: Computed Equilibrium Structures of the Cyanoacetylene Dimer (All Values in Angstroms)

method	basis set	$r(\text{H}-\text{C})$	$r(\text{C}\equiv\text{C})$	$r(\text{C}-\text{C})$	$r(\text{C}\equiv\text{N})$	$r(\text{N}-\text{H})$	$r(\text{H}-\text{C})$	$r(\text{C}\equiv\text{C})$	$r(\text{C}-\text{C})$	$r(\text{C}\equiv\text{N})$
SCF	I	1.0584	1.1852	1.3902	1.1353	2.3623	1.0622	1.1866	1.3905	1.1366
	II	1.0571	1.1777	1.3861	1.1269	2.3871	1.0607	1.1792	1.3863	1.1279
	III	1.0563	1.1782	1.3876	1.1278	2.3988	1.0597	1.1797	1.3880	1.1290
B3LYP	I	1.0673	1.2096	1.3715	1.1647	2.2082	1.0736	1.2113	1.3721	1.1663
	II	1.0646	1.2001	1.3676	1.1548	2.2602	1.0706	1.2018	1.3683	1.1563
	III	1.0640	1.2004	1.3683	1.1553	2.2662	1.0699	1.2020	1.3690	1.1569
MP2	I	1.0645	1.2235	1.3754	1.1869	2.2433	1.0694	1.2249	1.3762	1.1878
	II	1.0632	1.2118	1.3687	1.1740	2.2837	1.0680	1.2132	1.3695	1.1753
	III	1.0656	1.2159	1.3712	1.1776	2.2532	1.0710	1.2175	1.3720	1.1792
expt ^a						2.266				

^a Reference 29; under the assumption of a frozen monomer geometry.

$\text{C}\equiv\text{C}$ and $\text{C}\equiv\text{N}$ triple bond lengths, the MP2 values are larger than the B3LYP values by about 0.02 Å. Comparison of our MP2 and B3LYP optimized geometries to the more accurate monomer structures reported by Botschwina,^{32,54} who applied the coupled electron pair approximation (CEPA) in combination with empirical corrections based on experimental rotational constants, helps to assess the errors to be expected for the larger clusters. In case of the triple bond lengths, the CEPA values are bracketed by the B3LYP and MP2 values. With both B3LYP and MP2, the length of the C–C single bond in cyanoacetylene is quite accurately described. Also the MP2 and B3LYP H–C bond lengths agree quite well with the corresponding CEPA results. Evidently, at each level of approximation, all the errors appearing in the monomer geometries will unavoidably be reencountered in the equilibrium structures of the larger linear and cyclic clusters.

Dimers. For all the tables and figures pertaining to the results obtained for the linear oligomers, we assumed that the molecules are arranged with the non-hydrogen-bonded H–C group at the left end of the cluster as shown in Figure 1, and a consecutive ordering of the bonds or numbering of the molecules from the left to the right. The computed equilibrium structures of the linear hydrogen cyanide dimer and the cyanoacetylene dimer are shown in Tables 3 and 4. Close inspection of the computed modifications of the intramolecular bonds lengths in the dimers clearly demonstrates that, with the exception of the hydrogen-bonded H–C group, all other bond length changes with respect to the corresponding monomer structures are below 0.002 Å. As usual, the intermolecular distance $r(\text{N} \cdots \text{H})$ is considerably overestimated at the SCF level (by about 0.1 Å). With the two larger basis sets, II and III, the B3LYP and MP2 optimized intermolecular distances agree within a few hundredth of an angstrom or even better, for both the hydrogen cyanide and the cyanoacetylene dimers, and are also in acceptable agreement with the experimental values. At each theoretical level, the predicted intermolecular distance is slightly larger for the case of the cyanoacetylene dimer (by about 0.02–0.04 Å at the MP2 and B3LYP levels, by about 0.06 Å at the SCF level) than for the hydrogen cyanide dimer. This appears to be in line with the experimental results.^{29,56}

Linear Trimers and Higher Linear Oligomers. Because of the very small intramolecular geometry relaxations observed in the computed dimer structures, because of obvious space restrictions, and because the main qualitative features turned out not to depend too sensitively on the level of approximation chosen, only the trends in the intramolecular H–C and the intermolecular N \cdots H distances will be discussed for the linear trimer and the higher linear oligomers. The fully optimized structures and other calculated results of all the linear and cyclic hydrogen cyanide and cyanoacetylene clusters are, however, available upon request from the author.

TABLE 5: Computed H–C and N \cdots H Equilibrium Bond Lengths of Linear Hydrogen Cyanide Oligomers (All Values in Angstroms)

basis set	B3LYP			MP2		
	I	II	III	I	II	III
$r(\text{H}-\text{C})$						
trimer	1.0701	1.0684	1.0675	1.0657	1.0654	1.0675
	1.0791	1.0770	1.0759	1.0724	1.0720	1.0748
tetramer	1.0786	1.0767	1.0756	1.0721	1.0719	1.0746
	1.0702	1.0685	1.0676	1.0658	1.0655	
pentamer	1.0799	1.0778	1.0767	1.0730	1.0727	
	1.0819	1.0795	1.0784	1.0743	1.0739	
hexamer	1.0794	1.0774	1.0763	1.0726	1.0724	
	1.0702	1.0685	1.0676	1.0658		
	1.0803	1.0781	1.0771	1.0732		
	1.0829	1.0805	1.0794	1.0749		
	1.0828	1.0804	1.0793	1.0748		
	1.0797	1.0777	1.0766	1.0727		
	1.0703	1.0685	1.0677	1.0659		
	1.0804	1.0783	1.0772	1.0733		
	1.0834	1.0809	1.0798	1.0752		
	1.0840	1.0815	1.0804	1.0755		
	1.0832	1.0808	1.0796	1.0751		
	1.0798	1.0778	1.0767	1.0728		
$r(\text{N} \cdots \text{H})$						
trimer	2.1210	2.1661	2.1704	2.1762	2.2098	2.1801
	2.1289	2.1765	2.1806	2.1825	2.2187	2.1894
tetramer	2.1062	2.1490	2.1529	2.1642	2.1942	
	2.0711	2.1124	2.1163	2.1347	2.1621	
pentamer	2.1160	2.1612	2.1653	2.1720	2.2061	
	2.1008	2.1427	2.1466	2.1600		
hexamer	2.0547	2.0943	2.0980	2.1215		
	2.0565	2.0966	2.1005	2.1231		
	2.1112	2.1556	2.1598	2.1682		
	2.0983	2.1399	2.1438	2.1581		
	2.0486	2.0874	2.0912	2.1168		
	2.0394	2.0785	2.0818	2.1095		
	2.0510	2.0904	2.0944	2.1187		
	2.1090	2.1532	2.1572	2.1665		

The B3LYP and MP2 optimized H–C and N \cdots H distances of the linear hydrogen cyanide clusters from the trimer to the hexamer are compiled in Table 5. The computed SCF data have been omitted in this case, however, for similar detailed listings of SCF and MP2 (up to the tetramer) data the reader may compare with Table 2 of ref 23. Instead in Figure 2, the relaxations of the H–C and N \cdots H distances with increasing cluster size as obtained at the SCF level with basis set I are shown graphically for the case of linear hydrogen cyanide clusters for $n = 1-10$ and compared to the corresponding MP2 and B3LYP results for $n = 1-6$ using the same basis set.

Selected SCF and the B3LYP and MP2 optimized H–C and N \cdots H distances of linear cyanoacetylene clusters are given in Table 6. An analogue to Figure 2 for the case of the linear cyanoacetylene clusters up to the hexamer is provided in Figure 3. The data of Tables 5 and 6 and Figures 2 and 3 very clearly illustrate the almost identical qualitative convergence pattern

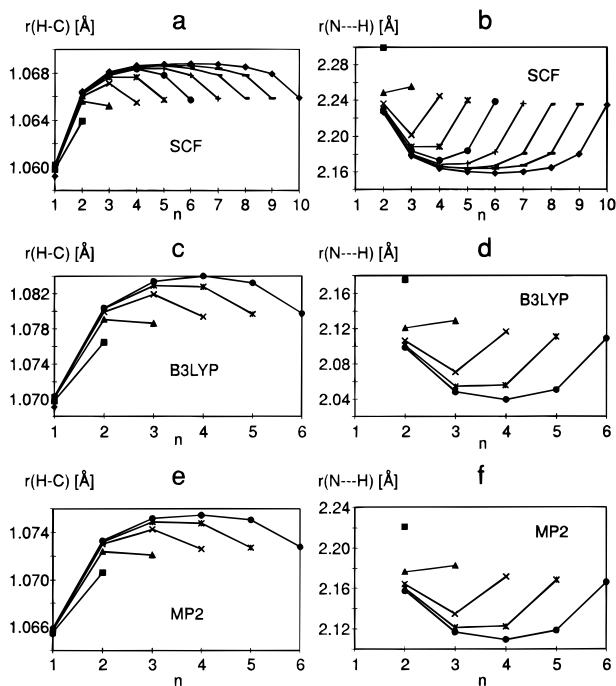


Figure 2. Trends in $r(\text{H}-\text{C})$ and $r(\text{N} \cdots \text{H})$ distances in linear hydrogen cyanide clusters, $(\text{HCN})_n$, with increasing cluster size n as obtained at the SCF (a, b), B3LYP (c, d), and MP2 (e, f) level, respectively. Distances belonging to the same oligomer are marked by identical symbols and connected by lines.

TABLE 6: Computed H-C and N...H Equilibrium Bond Lengths of Linear Cyanoacetylene Oligomers (All Values in Angstroms)

basis set	SCF		B3LYP		MP2	
	I	II	I	II	I	II
$r(\text{H}-\text{C})$						
trimer	1.0585	1.0674	1.0647	1.0642	1.0646	1.0633
	1.0630	1.0751	1.0720	1.0712	1.0704	1.0689
tetramer	1.0628	1.0749	1.0717	1.0710	1.0702	1.0687
	1.0585	1.0675	1.0647	1.0642	1.0647	
pentamer	1.0631	1.0755	1.0723	1.0715	1.0707	
	1.0635	1.0766	1.0732	1.0725	1.0714	
hexamer	1.0629	1.0752	1.0720	1.0713	1.0704	
	1.0585	1.0675			1.0647	
pentamer	1.0632	1.0757			1.0708	
	1.0636	1.0770			1.0717	
hexamer	1.0636	1.0769			1.0716	
	1.0630	1.0753			1.0705	
hexamer	1.0585	1.0675			1.0647	
	1.0633	1.0757			1.0708	
hexamer	1.0640	1.0772			1.0717	
	1.0641	1.0774			1.0719	
hexamer	1.0639	1.0771			1.0717	
	1.0631	1.0753			1.0705	
$r(\text{N} \cdots \text{H})$						
trimer	2.3295	2.1721	2.2242	2.2298	2.2176	2.2565
	2.3326	2.1765	2.2285	2.2333	2.2202	2.2606
tetramer	2.3236	2.1645	2.2172	2.2207	2.2123	
	2.2986	2.1387	2.1897	2.1955	2.1923	
pentamer	2.3271	2.1686	2.2219	2.2262	2.2153	
	2.3216	2.1616			2.2101	
hexamer	2.2910	2.1308			2.1867	
	2.2916	2.1313			2.1867	
hexamer	2.3252	2.1662			2.2134	
	2.3197	2.1613			2.2094	
hexamer	2.2892	2.1277			2.1844	
	2.2845	2.1225			2.1809	
hexamer	2.2898	2.1284			2.1849	
	2.3233	2.1656			2.2124	

from the structure of the isolated hydrogen cyanide or cyanoacetylene monomers to that of the monomers embedded in

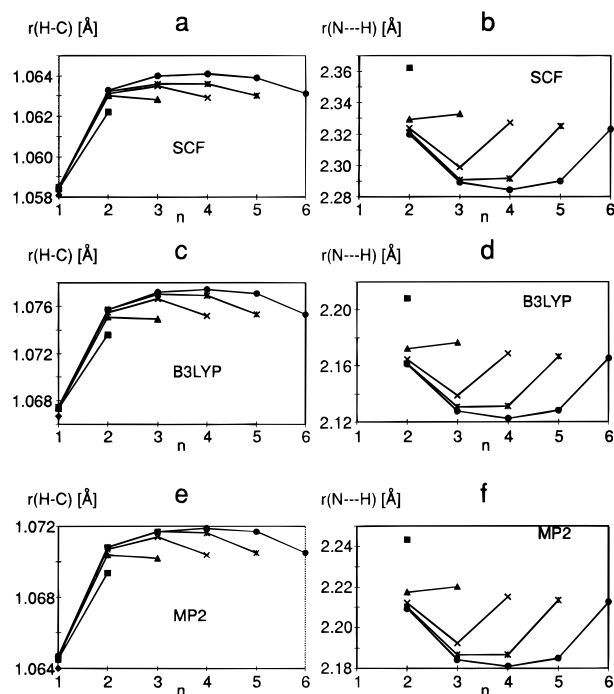


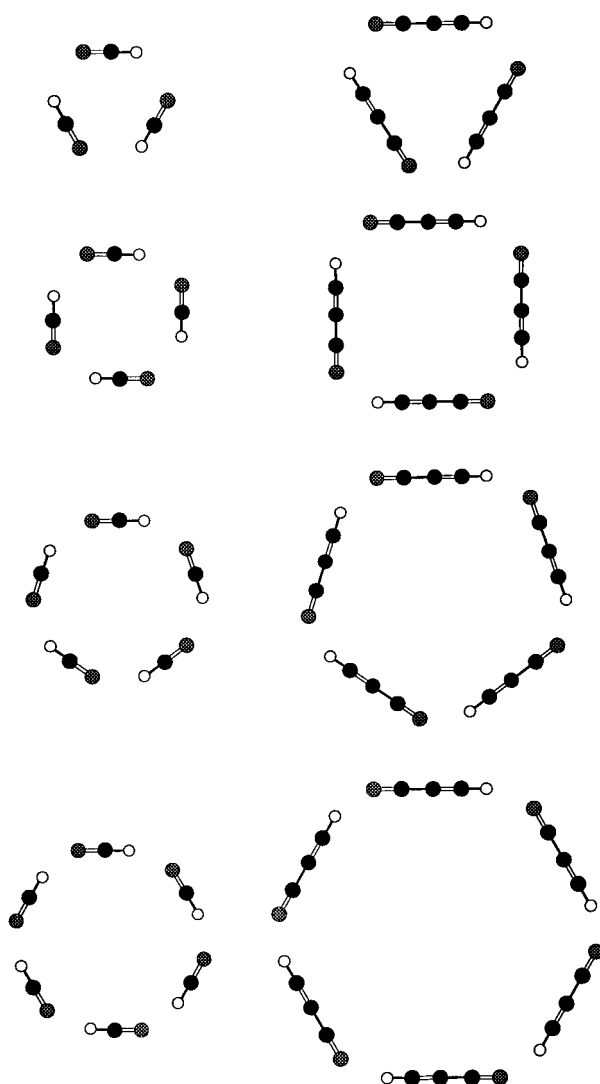
Figure 3. Trends in $r(\text{H}-\text{C})$ and $r(\text{N} \cdots \text{H})$ distances in linear cyanoacetylene clusters, $(\text{HC}_3\text{N})_n$, with increasing cluster size n as obtained at the SCF (a, b), B3LYP (c, d), and MP2 (e, f) level, respectively. Distances belonging to the same oligomer are marked by identical symbols and connected by lines.

extended hydrogen-bonded chains. Simultaneously, the qualitatively very similar description at the three levels of approximation becomes apparent. It is immediately visible that, upon increasing the cluster size, the length of the non-hydrogen-bonded, *free* H-C bond converges very fast. Similarly, the structural characteristics of the hydrogen bond at the opposite edge of the linear clusters are close to convergence for the hexamers, whereas convergence to the bulk properties in the center of the linear clusters is somewhat slower. Figures 2 and 3 also demonstrate convincingly the coupling between the H-C and the N...H distances of the various N...H-C hydrogen bonds in these species. This may serve as an illustration for the well-known feature that a shortening of the H...Y intermolecular bond occurs, whenever the X-H bond of a hydrogen bond X-H...Y is elongated or vice versa.

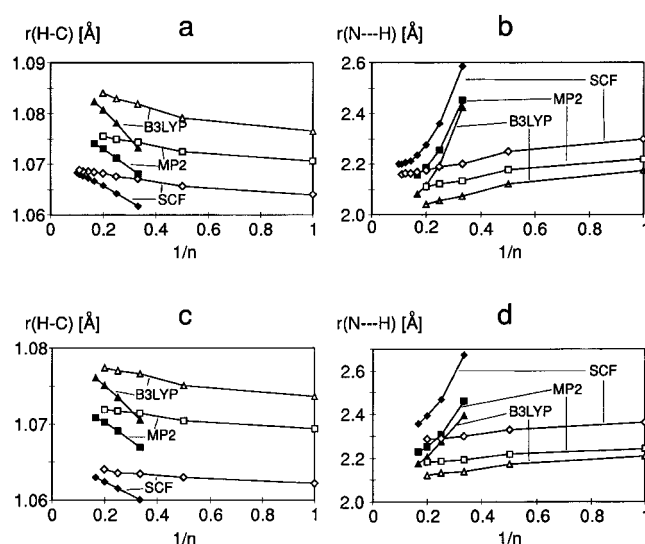
Analyzing the structural data more quantitatively, we observe that the H-C bond length increase from the monomer to the center molecules in the hydrogen cyanide hexamer amounts to about 0.01 Å at the SCF and MP2 levels using basis set I, whereas the corresponding B3LYP value is 0.015 Å. A similar trend is observed for cyanoacetylene clusters with computed C-H bond length elongations of 0.006, 0.008, and 0.011 Å at the SCF, MP2, and B3LYP levels, respectively. Because of the well-established correlation between bond lengths and the corresponding stretching frequencies, the larger increase predicted using the density functional technique must have consequences for the theoretical vibrational spectra to be discussed later on. With all three methods the predicted reduction of the intermolecular distance $r(\text{N} \cdots \text{H})$ from the dimer to the hexamer center is slightly larger than 0.12 Å for the hydrogen cyanide case. This can be compared to the experimental reduction from the dimer⁵⁶ to the crystal¹⁷ which under the assumption of frozen monomers amounts to about 0.10 Å. For the cyanoacetylenes, the corresponding computed shortening of $r(\text{N} \cdots \text{H})$ is smaller and varies between 0.06 and 0.09 Å in reasonable agreement with the experimental^{28,29} value of 0.05 Å.

TABLE 7: Computed H-C and N-H Equilibrium Bond Lengths (angstroms) and Intermolecular Bond Angles (degrees) of Cyclic Hydrogen Cyanide Oligomers

basis set		B3LYP			MP2		
		I	II	III	I	II	III
trimer	$r(\text{H}-\text{C})$	1.0732	1.0709	1.0702	1.0681	1.0677	1.0700
	$r(\text{N} \cdots \text{H})$	2.4222	2.5272	2.5101	2.4514	2.5010	2.4517
	$\angle \text{C}-\text{H} \cdots \text{N}$	125.5	121.1	122.7	122.3	119.5	122.2
	$\angle \text{N} \cdots \text{H}-\text{C}$	117.8	121.9	120.1	120.6	123.4	120.8
tetramer	$r(\text{H}-\text{C})$	1.0781	1.0752	1.0743	1.0712	1.0710	
	$r(\text{N} \cdots \text{H})$	2.1936	2.2673	2.2597	2.2564	1.2722	
	$\angle \text{C}-\text{H} \cdots \text{N}$	143.9	140.0	141.4	142.2	140.2	
	$\angle \text{N} \cdots \text{H}-\text{C}$	129.5	133.3	131.7	130.7	133.1	
pentamer	$r(\text{H}-\text{C})$	1.0807	1.0777	1.0769	1.0731		
	$r(\text{N} \cdots \text{H})$	2.1150	2.1733	2.1670	2.1861		
	$\angle \text{C}-\text{H} \cdots \text{N}$	152.7	149.0	150.8	151.8		
	$\angle \text{N} \cdots \text{H}-\text{C}$	138.2	142.0	140.1	138.8		
hexamer	$r(\text{H}-\text{C})$	1.0823	1.0794	1.0785	1.0741		
	$r(\text{N} \cdots \text{H})$	2.0800	2.1279	2.1254	2.1558		
	$\angle \text{C}-\text{H} \cdots \text{N}$	158.0	154.9	156.3	157.3		
	$\angle \text{N} \cdots \text{H}-\text{C}$	144.6	147.9	146.4	145.0		

**Figure 4.** Schematic representation of cyclic hydrogen cyanide and cyanoacetylene clusters.

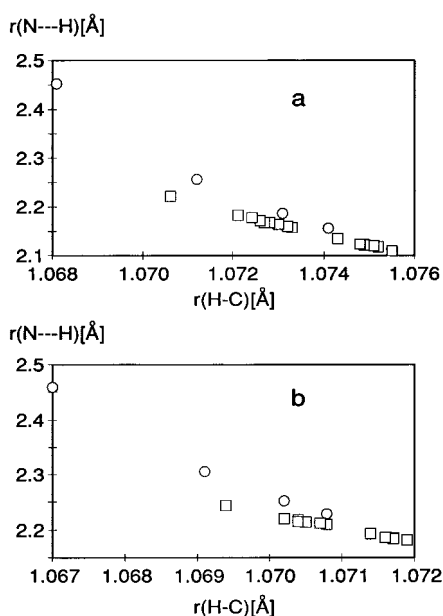
Cyclic Trimers and Higher Cyclic Oligomers. The structures of the cyclic C_{nh} -symmetric hydrogen cyanide and cyanoacetylene clusters are sketched in Figure 4. All these species are true minima on the potential energy surface, as the vibrational analysis proved a posteriori. As with the linear clusters, we do not report the entire sets of intramolecular structural relaxations but concentrate on the H-C and the N-

**Figure 5.** Plots of $r(\text{H}-\text{C})$ and $r(\text{N}-\text{H})$ distances in cyclic and linear (from the center molecule) hydrogen cyanide, $(\text{HCN})_n$ (a, b), and cyanoacetylene, $(\text{HC}_3\text{N})_n$ (c, d) clusters vs $1/n$, as obtained at the SCF, B3LYP, and MP2 levels, respectively. Distances belonging to the same oligomer are marked by identical symbols and connected by lines.

-H bond lengths and on the two intermolecular bond angles, $\angle \text{C}-\text{H} \cdots \text{N}$ and $\angle \text{H} \cdots \text{N}-\text{C}$. These are shown in Tables 7 and 8 for the cyclic hydrogen cyanide and cyanoacetylene clusters, respectively. We mention, however, that the computed intramolecular distortions from linearity in the case of the hydrogen cyanide molecules amount to about $2.5 \pm 1^\circ$ in all rings at all theoretical levels. Similarly, for the cyanoacetylene molecules in the cyclic clusters, the distortions of the individual intramolecular bond angles are always smaller than 3° and hence can be considered as negligibly small. Additionally, in Figure 5, the H-C and N-H bond lengths of the cyclic oligomers are plotted versus $1/n$ together with the corresponding H-C and N-H distances extracted from the central molecules of the linear clusters. In that way, the convergence of the intra- and intermolecular structure of the linear and cyclic oligomers to the same bulk limit is nicely illustrated. As a final point in the discussion of structural data, the smooth correlation between the H-C and the corresponding N-H distances of the different N-H-C hydrogen bonds is shown explicitly in Figure 6 for all the MP2-optimized structures of linear and cyclic hydrogen cyanide and cyanoacetylene clusters as obtained with basis set I. Analogous pictures of the corresponding SCF or B3LYP correlations are qualitatively very similar and hence omitted.

TABLE 8: Computed H–C and N–H Equilibrium Bond Lengths (angstroms) and Bond Angles (deg) of Cyclic Cyanoacetylene Oligomers

basis set		SCF	B3LYP			MP2	
		I	I	II	III	I	II
trimer	$r(\text{H}-\text{C})$	1.0601	1.0705	1.0673	1.0677	1.0670	1.0656
	$r(\text{N} \cdots \text{H})$	2.6723	2.3953	2.5665	2.5627	2.4594	2.4748
	$\angle \text{C}-\text{H} \cdots \text{N}$	124.6	125.9	125.9	126.4	125.6	126.5
	$\angle \text{N} \cdots \text{H}-\text{C}$	119.8	119.6	120.9	120.1	119.8	119.0
tetramer	$r(\text{H}-\text{C})$	1.0615	1.0735	1.0701	1.0695	1.0691	
	$r(\text{N} \cdots \text{H})$	2.4678	2.2747	2.3397	2.3389	2.3052	
	$\angle \text{C}-\text{H} \cdots \text{N}$	140.3	144.0	142.5	143.1	143.9	
	$\angle \text{N} \cdots \text{H}-\text{C}$	133.8	131.1	134.0	133.2	131.2	
pentamer	$r(\text{H}-\text{C})$	1.0624	1.0751			1.0702	
	$r(\text{N} \cdots \text{H})$	2.3929	2.2059			2.2530	
	$\angle \text{C}-\text{H} \cdots \text{N}$	149.2	153.0			152.3	
	$\angle \text{N} \cdots \text{H}-\text{C}$	142.4	140.1			139.2	
hexamer	$r(\text{H}-\text{C})$	1.0630	1.0760			1.0708	
	$r(\text{N} \cdots \text{H})$	2.3551	2.1759			2.2281	
	$\angle \text{C}-\text{H} \cdots \text{N}$	154.7	158.0			157.7	
	$\angle \text{N} \cdots \text{H}-\text{C}$	148.5	146.6			145.5	

**Figure 6.** Plots of $r(\text{N} \cdots \text{H})$ vs $r(\text{H}-\text{C})$ in linear and cyclic hydrogen cyanide $(\text{HCN})_n$ (a) and cyanoacetylene $(\text{HC}_3\text{N})_n$ (b) clusters. Circles are for cyclic structures, squares for linear clusters.

Energetics

In Table 9, the total stabilization energies, $\Delta E_{\text{total}}(n)$, of the linear and cyclic hydrogen cyanide clusters, defined as

$$\Delta E_{\text{total}}(n) = E(n) - nE(1) \quad (1)$$

are compiled together with the corresponding zero-point energy (ZPE) corrected values. Table 10 contains the analogous data sets for the cyanoacetylene clusters.

In case of the dimers, we observe that the binding energies of the hydrogen cyanide dimer and of the cyanoacetylene dimer are very similar indeed. Whereas the ΔE value is still slightly more negative for the hydrogen cyanide dimer, the ZPE corrections narrow the difference considerably. In the case of the MP2 results with basis set II and III, both dimers are equally stable. To assess the eventual influence of the well-known basis set superposition error (BSSE), we have evaluated that quantity within the framework of the counterpoise procedure.⁵⁷ This was done at the MP2 level only. Whereas this correction is still about 1 kcal/mol for basis set I, it amounts to only 0.3 and 0.1 kcal/mol for basis sets II and III, respectively, for both

dimers. The MP2 stabilization energy of the hydrogen cyanide dimer reported in this work (−4.5 kcal/mol without and about −3.7 kcal/mol with ZPE correction as obtained with basis set III) agree quite well with our earlier, methodically superior coupled pair functional (CPF) and averaged coupled pair functional (ACPF) results^{18,19} and with the corresponding experimental results of −4.5⁵⁶ and −3.8⁵⁸ kcal/mol, respectively. The predicted MP2 stabilization energy of the cyanoacetylene dimer of −4.2 kcal/mol (−3.7 kcal/mol with ZPE correction) is hence believed to be reliable. The SCF and B3LYP dimer stabilization energies as obtained with basis sets II and III are, in general, lower in absolute value than the MP2 values.

Turning to the trimers, we observe that the computed relative stability of linear and cyclic aggregates depends quite sensitively on the level of approximation. The SCF calculations and even more so the B3LYP approach predict that the linear trimer is distinctly more stable than the cyclic trimer, quite independent of the basis set applied and with or without the ZPE correction. In contrary, the MP2 stabilization energies of cyclic and linear trimers are very close. With the largest basis set the balance is even tilted in favor of the cyclic structure in the case of hydrogen cyanide. The computed energy difference is, however, too small to permit a conclusive statement as to which of the two trimer structures is the more stable. With our previous ACPF computations,²² a small ZPE-corrected energy difference of 0.5 kcal/mol in favor of the linear configuration was obtained. Regrettably, the MP2 vibrational analysis of the cyanoacetylene trimers with basis set II and even the MP2 geometry optimization with basis set III surpassed our computational resources. The MP2 basis set I results point, however, to a slight preference for the cyclic structure. The accurate prediction of the energy difference between cyclic and linear trimers is actually a quite demanding problem since different sections of the intermolecular energy surfaces are probed. At all levels of approximation, the hydrogen cyanide trimers are found to be more strongly bound than the cyanoacetylene trimers.

The relative stability of linear and cyclic structures is still quite close for the tetramers. At the MP2 level, we obtain a difference of about 1 kcal/mol in favor of the cyclic structures. From the pentamers on, the one additional hydrogen bond present in the cyclic C_{nh} structures suffices to render the corresponding linear structures as the less stable aggregates, in agreement with previous SCF investigations.¹⁶ The trends observed for the stabilization energies of the larger linear and cyclic clusters can be analyzed by defining averaged binding energies per hydrogen bond^{59,60} as

TABLE 9: Total Stabilization Energies and Zero-Point Energy Corrected Stabilization Energies of Linear and Cyclic Hydrogen Cyanide Clusters (All Values in kcal/mol)

basis set <i>n</i>	SCF			B3LYP			MP2		
	I	II	III	I	II	III	I	II	III
Linear									
2	-4.7 ^a	-4.4	-4.2	-5.2	-4.4	-4.2	-5.3 (-4.3) ^b	-4.6 (-4.3)	-4.6 (-4.5)
	-3.8	-3.6	-3.4	-4.1	-3.6	-3.4	-4.2	-3.8	-3.8
3	-10.6	-9.8	-9.4	-11.6	-10.0	-9.6	-11.6	-10.3	-10.3
	-9.5	-8.2	-7.8	-9.5	-8.3	-7.9	-9.5	-8.7	-8.6
4	-16.8	-15.6	-15.0	-18.5	-16.0	-15.4	-18.4	-16.3	
	-14.0	-13.2	-12.6	-15.3	-13.5	-12.9	-15.1		
5	-23.2	-21.6	-20.7	-25.6	-22.2	-21.4	-25.2		
	-19.5	-18.4	-17.5	-21.2	-18.8	-18.0	-20.9		
6	-29.7	-27.7	-26.6	-32.8	-28.5	-27.5	-32.2		
	-25.0	-23.6	-22.5	-27.3	-24.2	-23.2	-26.7		
7	-36.3								
	-30.6								
8	-42.8								
	-36.1								
9	-49.4								
	-41.8								
10	-56.0								
	-47.4								
Cyclic									
3	-10.0	-8.7	-8.7	-10.3	-8.3	-8.4	-11.1	-10.1	-10.5
	-8.6	-7.3	-7.3	-8.7	-7.0	-6.9	-9.6	-8.7	-9.0
4	-18.1	-16.3	-16.0	-19.4	-16.3	-16.1	-19.6	-17.8	
	-15.5	-13.9	-13.6	-16.6	-13.9	-13.6	-16.9		
5	-25.9	-23.8	-23.1	-28.2	-24.3	-23.7	-27.8		
	-22.2	-20.4	-19.7	-24.1	-20.7	-20.1	-23.9		
6	-33.5	-31.0	-29.9	-36.6	-31.8	-31.0	-35.8		
	-28.7	-26.6	-25.6	-31.4	-27.3	-26.5	-30.3		
7	-40.8								
	-35.0								
8	-48.1								
	-41.2								
9	-55.2								
	-47.2								
10	-62.2								
	-53.2								

^a The first entry is the stabilization energy; the second entry (in italics) is the ZPE-corrected stabilization energy. ^b BSSE-corrected stabilization energies in parentheses.

$$\Delta E_a(n) = E(n) - E(n-1) - E(1) \quad (2)$$

or as

$$\Delta E_b(n) = (E(n) - nE(1))/m \quad (3)$$

where $m = n$ for cyclic, and $m = n - 1$ for linear clusters. As an illustration, plots of the SCF and MP2 (basis set I) $\Delta E_a(n)$ and $\Delta E_b(n)$ values versus $1/n$ are shown in Figures 7 and 8 for the cyclic and linear hydrogen cyanide and cyanoacetylene complexes, respectively. Fully analogous figures for the B3LYP data and for the corresponding ZPE-corrected quantities at all three levels of approximation look very similar and hence are not shown explicitly. In all cases, the four different curves must necessarily converge to the same limit that characterizes the binding energy of a C–H hydrogen bond embedded in infinitely extended hydrogen cyanide or cyanoacetylene chains. Rather than to extend the cluster calculations to still larger oligomers, it seems admissible to use a simple graphical extrapolation, in order to obtain approximate values for $n = \infty$. In case of the more reliable MP2(I) values of Figures 7b and 8b, we thus arrive at limiting stabilization energies of about -7 kcal/mol and of about -5.9 kcal/mol for hydrogen cyanide and cyanoacetylene molecules, respectively. More precise values could be obtained by explicit consideration of translational symmetry, as has already been done previously at the SCF²⁶ and MP2²⁵ levels for hydrogen cyanide polymers. In this work, this extra task

was, however, not carried out. In view of the fact that the MP2-(I) stabilization energies of hydrogen cyanide and cyanoacetylene dimers were much closer, -5.3 and -4.9 kcal/mol, respectively, we observe that the non-nearest-neighbor interaction energies are considerably larger in the hydrogen cyanide case.

Vibrational Spectra

Rather than dwell in detail on the entire theoretical vibrational spectra of all the clusters treated, we restrict ourselves to a discussion of the C–H stretching region only, mainly because almost all the available experimental data originate from an analysis of that energy region. Complete harmonic vibrational spectra for the hydrogen cyanide dimer and the two types of trimers as calculated at a correlated (ACPF) level were already presented previously.²²

In Table 11, the harmonic $\nu(\text{C–H})$ stretching frequencies of the hydrogen cyanide monomers which were computed at the different levels of approximation are compiled together with the theoretical shifts of the C–H stretching frequencies in the linear and cyclic hydrogen cyanide clusters relative to the monomer frequency. Available information on the experimental C–H stretching fundamentals is included, too. Table 12 contains the corresponding data for cyanoacetylene clusters. Moreover, the computed monomer infrared intensities and the intensity enhancement factors of the cluster C–H stretching vibrations with respect to the monomer intensities are reported

TABLE 10: Total Stabilization Energies and Zero-Point Energy Corrected Stabilization Energies of Linear and Cyclic Cyanoacetylene Clusters (All Values in kcal/mol)

basis set n	SCF			B3LYP			MP2		
	I	II	III	I	II	III	I	II	III
Linear									
2	-4.0 ^a	-3.7	-3.6	-4.6	-4.0	-3.8	-4.9 (-4.1) ^b	-4.3 (-4.0)	-4.3 (-4.2)
3	-3.4	-3.2	-3.1	-3.9	-3.4	-3.4	-4.1	-3.8	-3.8
4	-8.6	-7.9	-7.7	-10.0	-8.6	-8.2	-10.5	-9.2	
5	-7.4	-6.9	-6.7	-8.5	-7.4	-7.9	-8.8		
6	-13.4	-12.4	-12.0	-15.6	-13.5	-12.9	-16.2		
	-11.6	-10.8		-13.3	-11.7				
5	-18.2			-21.3			-22.0		
	-15.9			-18.3					
6	-23.1			-27.0			-27.8		
	-20.2			-23.2					
Cyclic									
3	-7.8	-6.5	-6.4	-8.9	-6.8	-6.6	-10.5	-9.5	
	-6.8	-5.6	-5.6	-7.5	-5.8	-5.7	-9.3		
4	-13.9	-12.1	-11.9	-16.2	-13.2	-12.8	-17.3		
	-12.2	-10.6		-14.0	-11.5				
5	-19.7			-23.0			-24.0		
	-17.3			-20.1					
6	-25.3			-29.6			-30.5		
	-22.3			-25.9					

^a The first entry is the stabilization energy, the second entry (in italics) is the ZPE-corrected stabilization energy. ^b BSSE corrected stabilization energies in parentheses.

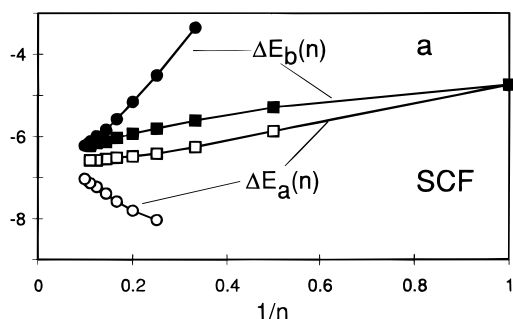
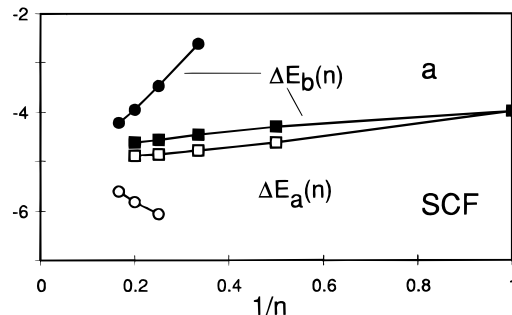
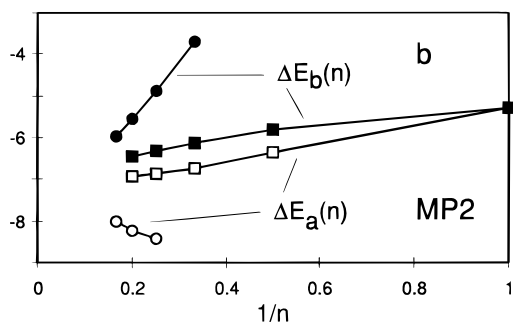
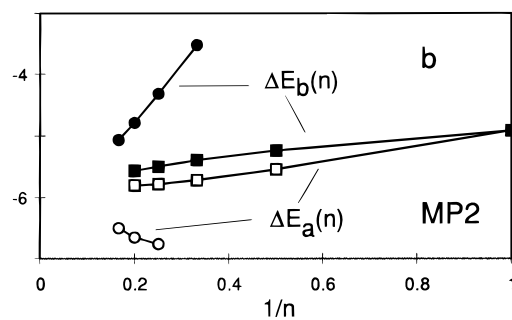
E [kcal/mol]**E [kcal/mol]****E [kcal/mol]****E [kcal/mol]**

Figure 7. Plots of $\Delta E_a(n)$ and $\Delta E_b(n)$ vs $1/n$ for linear and cyclic hydrogen cyanide oligomers as obtained at the SCF (a) and MP2 (b) levels. n is the number of hydrogen bonds in the cluster. Open symbols $\Delta E_a(n)$; filled symbols $\Delta E_b(n)$; circles, cyclic structures; squares, linear structures.

Figure 8. Plots of $\Delta E_a(n)$ and $\Delta E_b(n)$ vs $1/n$ for linear and cyclic cyanoacetylene oligomers as obtained at the SCF (a) and MP2 (b) levels. n is the number of hydrogen bonds in the cluster. Open symbols $\Delta E_a(n)$; filled symbols $\Delta E_b(n)$; circles, cyclic structures; squares, linear structures.

in Table 13 for the hydrogen cyanide clusters and in Table 14 for the cyanoacetylene clusters.

In case of the hydrogen cyanide dimer the experimentally determined shifts⁵ of the two C–H stretching frequencies are -4 cm^{-1} for the *free* C–H group and -70 cm^{-1} for the hydrogen-bonded C–H group. At the SCF level, the theoretical shifts for the hydrogen-bonded C–H stretch are with about -60 cm^{-1} slightly below, the MP2 predictions (-74 to -87 cm^{-1}) somewhat above the experimental value, the B3LYP values

(-94 to -101 cm^{-1}) even more so. These trends are reencountered when comparing the experimental shifts for the linear trimer with the theoretical shifts and become more prominent for the larger clusters. The internal methodical comparison in the case of the cyclic trimer yields a similar picture, with the MP2 shifts between the SCF and B3LYP data. There, the experimental value of -38 cm^{-1} is, however, slightly larger in absolute value than most of the theoretical shifts.

In the case of the cyanoacetylene clusters, the experimentally determined shifts assigned to the hydrogen-bonded C–H

TABLE 11: Computed C–H Stretching Frequency in the Hydrogen Cyanide Monomer and the Relative Shifts of C–H Stretching Frequencies in Linear and Cyclic Hydrogen Cyanide Clusters^a

		SCF			B3LYP			MP2		
basis set	exp	I	II	III	I	II	III	I	II	III
Linear										
monomer	3312 ^b	3651	3616	3608	3476	3444	3436	3529	3496	3454
dimer	−4 ^c	−5	−5	−7	−4	−5	−3	−1	−3	−6
	−70 ^c	−61	−62	−61	−101	−98	−94	−74	−79	−87
trimer	−5 ^d	−6	−7	−9	−6	−7	−5	−2	−4	−7
		−74	−75	−72	−122	−119	−116	−90	−92	−106
	−99 ^d	−85	−85	−82	−140	−133	−130	−103	−103	−118
tetramer		−7	−8	−10	−7	−7	−6	−3		
		−81	−82	−81	−137	−133	−130	−100		
		−84	−85	−84	−140	−135	−132	−103		
		−106	−104	−103	−177	−166	−163	−129		
pentamer		−8	−9	−11	−7	−7	−6	−3		
		−84	−85	−83	−142	−137	−134	−102		
		−87	−88	−86	−145	−139	−136	−105		
		−103	−104	−101	−175	−167	−164	−126		
		−117	−116	−114	−198	−186	−183	−143		
hexamer		−8	−9	−11	−7	−8	−6	−4		
		−84	−87	−84	−144	−139	−136	−103		
		−88	−89	−87	−146	−141	−138	−106		
		−105	−106	−104	−180	−172	−169	−128		
		−112	−112	−110	−190	−180	−177	−136		
		−126	−124	−122	−214	−200	−196	−153		
Cyclic										
trimer	−38 ^d	−25	−24	−25	−43	−35	−37	−29	−29	−36
		−28	−27	−29	−49	−40	−42	−33	−33	−41
tetramer		−52	−52	−51	−104	−88	−88	−68		
		−57	−56	−55	−111	−93	−93	−73		
		−64	−62	−61	−125	−103	−104	−84		
pentamer		−73	−68	−69	−140	−122	−125	−94		
		−81	−75	−76	−153	−132	−135	−104		
		−89	−82	−83	−169	−145	−148	−116		
hexamer		−84	−82	−81	−158	−144	−144	−107		
		−88	−85	−84	−164	−148	−148	−111		
		−97	−93	−92	−180	−161	−161	−123		
		−105	−101	−100	−196	−174	−174	−134		

^a Frequencies and frequency shifts in cm^{−1}. ^b Fundamental frequency; the experimental harmonic frequency is 3442 cm^{−1}.⁶¹ ^c Reference 5.

stretches of the linear dimer, the linear trimer, and the cyclic trimer^{29,30} are −66, −80, and −33 cm^{−1}, all weaker than their counterparts in the corresponding hydrogen cyanide clusters. This is also true for all the calculated shifts, with exactly the same methodical trends as just discussed for the HCN clusters. In Figure 9a, a naive correlation between the experimental $\nu(\text{C–H})$ shifts and the calculated MP2 (basis set I) shifts up to the trimers is shown for the hydrogen cyanide and the cyanoacetylene clusters. Visual inspection immediately reveals that to a good approximation, both these correlations are very close to linear indeed. In Figure 9b, the corresponding correlation between the experimental and the theoretical SCF(I) shifts is shown for the case of the cyanoacetylene clusters. In this case the correlation also does not deviate substantially from linearity.

In Figure 10, the most intense infrared active C–H stretching frequencies of cyclic and linear hydrogen cyanide and cyanoacetylene clusters are plotted versus $1/n$, where n is the number of molecules in the cluster. Not unexpectedly, this figure tells us that (i) the intense frequencies of linear and cyclic clusters converge to the same limit and (ii) apart from an initial period (monomer, dimer), the $1/n$ behavior is again close to linear.

Definite experimental assignments for the C–H stretching vibrations of linear and cyclic vapor phase clusters larger than the trimers are not available, neither for the hydrogen cyanide nor for the cyanoacetylene clusters. An upper limit to the shifts that can reasonably be expected for all the conceivable C–H stretching frequencies in chains and rings of hydrogen cyanide and cyanoacetylene clusters is, however, provided by the

experimental C–H stretching frequency in the corresponding molecular crystals. The experimental C–H stretching frequency of hydrogen cyanide in the solid state⁶² is 3130 cm^{−1}. That corresponds to a shift of −182 cm^{−1} with respect to the HCN monomer. For cyanoacetylene, the $\nu(\text{C–H})$ shift from the vapor-phase monomer to the molecular crystal is −123 cm^{−1}.³⁴ Hence, the feature of smaller shifts in the cyanoacetylene clusters appears to be continued for the larger clusters as well, fully in line with the smaller overall reduction of the intermolecular distance or with the weaker interaction energy in the latter case. A rough extrapolation of the cluster frequencies (linear and cyclic) shown in Tables 11 and 12 and in Figure 10 to $n = \infty$ leads to theoretical differences between monomer and crystal frequencies of about −167, −212 and −304 cm^{−1} at the SCF, MP2, and B3LYP levels, respectively, for hydrogen cyanide, and to −93 and −194 cm^{−1} at the SCF and B3LYP levels for cyanoacetylenes. Thus, while the SCF and MP2 overall shifts are about of the correct magnitude, the B3LYP approach, although still qualitatively acceptable, overshoots significantly.

In their recent work, Yang et al.³⁰ observed several additional bands in the C–H stretching region, which they could not assign unambiguously. They could, however, show conclusively that all these bands originate necessarily from unpolar clusters. In Figure 9b, we have included three of these bands (bands 4, 5, and 7 of ref 30) which were found experimentally at 3272, 3265, and 3249 cm^{−1}, respectively. On the basis of the otherwise acceptable performance of the SCF results and given the fact that at least among the series of cyclic clusters, there is

TABLE 12: Computed C–H Stretching Frequency in the Cyanoacetylene Monomer and the Relative Shifts of C–H Stretching Frequencies in Linear and Cyclic Cyanoacetylene Clusters^a

		SCF			B3LYP			MP2		
basis set	exp	I	II	III	I	II	III	I	II	III
Linear										
monomer	3327 ^b	3637	3614	3606	3482	3460	3455	3531	3503	3460
dimer	−3 ^c	−2	−3	−3	−4	−4	−5	−4	−2	−4
	−66 ^c	−51	−49	−47	−94	−87	−86	−72	−67	−78
trimer	−3 ^d	−3	−3	−3	−5	−5	−5	−5		
		−57	−55	−53	−108	−100	−100	−82		
	−80 ^d	−61	−58	−56	−115	−105	−105	−86		
tetramer		−4	−3		−5	−5				
		−60	−58		−115	−105				
		−60	−59		−117	−107				
		−68	−67		−134	−122				
pentamer		−3			−6					
		−61			−116					
		−61			−118					
		−67			−135					
		−71			−142					
hexamer		−3			−6					
		−62			−117					
		−63			−119					
		−70			−137					
		−72			−140					
		−76			−148					
Cyclic										
trimer	−33 ^d	−19	−18	−18	−41	−34	−36	−33		
		−21	−19	−19	−44	−36	−37	−35		
tetramer		−37	−33	−	−83	−71				
		−38	−34		−85	−73				
		−40	−36		−89	−76				
pentamer		−48			−106					
		−50			−110					
		−53			−115					
hexamer		−56			−118					
		−57			−119					
		−59			−124					
		−61			−129					

^a Frequencies and frequency shifts in cm^{–1}. ^b Reference 35. ^c Reference 29. ^d Reference 30.

practically no other choice, we tentatively assigned them to the cyclic tetramer, pentamer, and hexamer.

The computed theoretical C–H stretching infrared intensities (see Tables 13 and 14) can be compared with experimental data for the case of the monomers and for the linear (HCN)₂ and (HCN)₃ clusters only. In the case of hydrogen cyanide and cyanoacetylene monomers, experimental values of 60 km/mol have been reported^{34,63} for both species. The theoretical intensities obtained in this work are, in general, larger, with MP2 values in the range of 66–78 km/mol for hydrogen cyanide and 84–89 km/mol for cyanoacetylene. The corresponding B3LYP values are slightly lower. The experimental intensity enhancement factors for the linear (HCN)₂⁵ and (HCN)₃⁴ clusters are about 4.0 and 7.5, respectively, in good qualitative agreement with the values reported in Table 13.

Analysis of the computed theoretical C–H stretching infrared intensities shows that, with increasing degree of oligomerization, the intensity of the lowest band of each linear oligomer increases continuously (scales with *n*), whereas the intensities of the remaining modes are either hardly modified if compared to the dimer, or even vanish, as, e.g., for the second lowest mode. This can be easily understood by recognizing that linear finite and infinite chains (regular polymers) behave approximately like vibrating strings. The *in-phase* vibration, where all C–H stretches move in the same direction and where consequently all the dipole moment derivatives add up, is bound to converge to the only infrared active *k* = 0 C–H stretching crystal vibration. All other phase combinations are optically forbidden in the crystal. A detailed illustration of this well-known

behavior has recently been given for the case of hydrogen fluoride chains.⁶⁴ In the case of the ringlike clusters, the *in-phase* mode that will converge to the *k* = 0 polymer mode is always infrared inactive for symmetry reasons. However, the second-lowest degenerate and strongly infrared active ring vibration must converge to the same limit. A further notable feature is the quite narrow energy range of the C–H stretching vibrations in the rings which, because of the absence of edge effects, gives also an indication of the width of the entire phonon branch in the crystals. In earlier lattice dynamical calculations¹⁸ a width of about 20–30 cm^{–1} was obtained from SCF-derived scaled force constants for the hydrogen cyanide chain, in good agreement with the hexamer SCF, MP2, and also the B3LYP data obtained in this work. Again, the splitting of the ring modes is distinctly smaller for the cyanoacetylene clusters and hence the corresponding C–H stretching phonon branch will presumably be narrower in that case.

Summary, Conclusions and Outlook

We have presented a systematic series of *ab initio* calculations on a variety of ground-state properties of linear and cyclic hydrogen cyanide and cyanoacetylene clusters. A very consistent picture emerges from this investigation. As far as the structural, energetic, and vibrational spectroscopic features are concerned, a qualitatively very similar aggregation behavior is observed. The intra- and intermolecular structures of chains and rings as well as the hydrogen-bond energies per molecule in chains and rings converge to the same, respective limits.

TABLE 13: Computed C–H Stretching Infrared Intensities of the Hydrogen Cyanide Monomer and Intensity Enhancement Factors of the C–H Stretchings in Linear and Cyclic Hydrogen Cyanide Clusters^a

basis set	SCF			B3LYP			MP2		
	I	II	III	I	II	III	I	II	III
Linear									
monomer	67	75	72	57	69	68	66	74	78
dimer	1.0	0.9	0.9	1.1	1.0	1.0	1.1	1.1	1.1
	4.2	3.7	3.7	6.8	5.3	5.3	5.2	4.5	4.6
trimer	1.0	1.0	1.0	1.2	1.1	1.1	1.2	1.1	1.1
	0.1	0.1	0.1	0.0	0.0	0.0	0.0	0.0	0.0
	9.8	8.6	8.5	17.5	13.4	13.3	13.0	11.0	11.3
tetramer	1.0	1.0	1.0	1.2	1.1	1.1	1.2		
	3.2	3.0	2.8	6.9	5.6	5.2	4.5		
	0.7	0.5	0.6	0.4	0.5	0.8	0.8		
	12.4	10.7	10.7	23.0	16.9	16.7	16.9		
pentamer	1.0	1.0	1.0	1.2	1.1	1.1	1.2		
	2.2	2.0	2.1	3.4	2.9	3.2	2.9		
	3.2	2.9	2.8	6.5	5.3	4.9	4.3		
	0.0	0.0	0.0	0.0	0.0	0.0	0.0		
	17.9	15.2	15.2	34.2	25.2	24.9	24.6		
hexamer	1.0	1.0	1.0	1.2	1.1	1.1	1.2		
	2.7	2.5	2.4	4.8	3.9	3.9	3.5		
	2.6	2.5	2.4	5.4	4.4	4.3	3.8		
	3.0	2.2	2.2	4.7	3.8	3.7	2.9		
	0.0	0.0	0.0	0.0	0.0	0.0	0.0		
	22.1	19.1	19.0	43.7	31.9	31.7	31.6		
Cyclic									
trimer ^b	3.9	3.6	3.7	5.2	4.2	4.2	4.6	4.5	4.4
	0.0	0.0	0.0	0.0	0.0	0.0	0.0	0.0	0.0
tetramer	0.0	0.0	0.0	0.0	0.0	0.0	0.0		
	8.9	7.5	7.8	15.9	11.7	12.1	12.5		
	0.0	0.0	0.0	0.0	0.0	0.0	0.0		
pentamer	0.0	0.0	0.0	0.0	0.0	0.0	0.0		
	15.9	13.5	13.7	30.8	22.4	23.3	22.9		
	0.0	0.0	0.0	0.0	0.0	0.0	0.0		
hexamer	0.0	0.0	0.0	0.0	0.0	0.0	0.0		
	0.0	0.0	0.0	0.0	0.0	0.0	0.0		
	25.3	20.3	20.3	47.2	34.8	35.6	34.1		
	0.0	0.0	0.0	0.0	0.0	0.0	0.0		

^a Monomer infrared intensities in km/mol. ^b The factor of 2 due to the degeneracy of the infrared active vibration in the cyclic clusters is included.

Similarly, the trends in the vibrational frequencies of larger chains and rings can be understood by accepting that they have to converge again to the same limit. The only quantitative difference between the ring- and chainlike hydrogen cyanide and cyanoacetylene clusters concerns the somewhat smaller non-nearest-neighbor contributions to the stabilization or interaction energies in the cyanoacetylene case and the consequences thereof, i.e., slightly larger intermolecular distances, slightly smaller C–H bond length elongations and hence smaller C–H stretching frequency shifts in the case of the cyanoacetylene clusters. Although with such extended molecules the use of the two-center multipole expansion may be questionable, the most simple rationalization for this behavior can be gained by considering the molecular dipole moments μ and the center-to-center distances R in the chains. The long range interaction, i.e., all non-nearest-neighbor interactions between the molecules must then to a good approximation behave like μ^2/R^3 , since all other attractive terms to the interaction energy, like quadrupole–quadrupole or dispersion contributions must have practically vanished. The computed dipole moment ratio between the cyanoacetylene and hydrogen cyanide monomers is about $4/3$ at all computational levels considered in this work. The ratio of the center-to-center intermolecular distances, however, amounts to about 1.6. The resultant long-range interaction energy ratio between nonneighboring molecules is hence approximately 0.4.

TABLE 14: Computed C–H Stretching Infrared Intensities of the Cyanoacetylene Monomer and Intensity Enhancement Factors of the C–H Stretchings in Linear and Cyclic Cyanoacetylene Clusters^a

basis set	SCF			B3LYP			MP2		
	I	II	III	I	II	III	I	II	III
Linear									
monomer	74	81	77	81	78	83	84	89	86
dimer	1.0	1.0	1.0	1.0	1.0	1.0	1.1	1.1	1.1
	4.7	4.1	4.2	7.2	6.1	6.1	6.0	5.5	5.7
trimer	1.0	1.0	1.0	1.1	1.1	1.1	1.1		
	0.2	0.2	0.1	0.3	0.3	0.2	0.3		
	10.5	9.1	9.2	17.1	14.0	14.3	13.7		
tetramer	1.0	1.0		1.1	1.1				
	3.9	3.3		6.1	4.9				
	1.6	2.1		4.4	4.0				
	11.6	9.4		18.2	14.5				
pentamer	1.0			1.1	-				
	2.9			5.7	-				
	3.4			6.3	-				
	0.0			0.0					
	17.4			28.4					
hexamer	1.0			1.1					
	3.4			6.0					
	3.6			6.3					
	2.7			4.1					
	0.0			0.0					
	20.5			35.9					
Cyclic									
trimer ^b	3.6	3.4	3.4	4.6	4.0	4.0	4.4		
	0.0	0.0	0.0	0.0	0.0	0.0	0.0		
	0.0	0.0		0.0	0.0				
	8.2	7.2		13.0	10.8				
	0.0	0.0		0.0	0.0				
pentamer	0.0			0.0	-				
	14.7			13.2	-				
	0.0			0.0					
hexamer	0.0			0.0					
	0.0			0.0					
	22.1			38.3					
	0.0			0.0					

^a Monomer infrared intensities in km/mol. ^b The factor of 2 due to the degeneracy of the infrared active vibration in the cyclic clusters is included.

As already noted in several previous investigations,^{3,16,18–26} the SCF results are surprisingly good for both types of hydrogen cyanide clusters and do not differ substantially from the MP2 results. From our calculations it appears that this finding is also valid for the cyanoacetylene clusters. The B3LYP approach, however, although qualitatively still acceptable and in some aspects (intramolecular geometries, interaction energies and other expectation values) clearly superior to the SCF results, overshoots in the description of one of the typical hydrogen-bond properties, i.e., the B3LYP computed shifts of the C–H stretching modes in the larger chains and rings are considerably overestimated. Similar results have been obtained in a number of recent evaluations^{65–72} of several variants of the more modern density functional techniques, where B3LYP emerged as one of the most promising variant for hydrogen-bond interactions, at least for dimers.

The statements just made concerning the performance of the different quantum chemical methods are unfortunately only valid for the strongly hydrogen-bonded configurations investigated in this work. Preliminary calculations on other selected sections of the intermolecular energy surfaces already showed that neither SCF nor B3LYP calculations provide satisfactory results. The theoretical treatment of other conceivable structures, such as, e.g., parallel, antiparallel, or T-shaped dimers with p-type hydrogen bonding, tetramers built from slipped parallel or antiparallel orientations between already preformed dimers, the

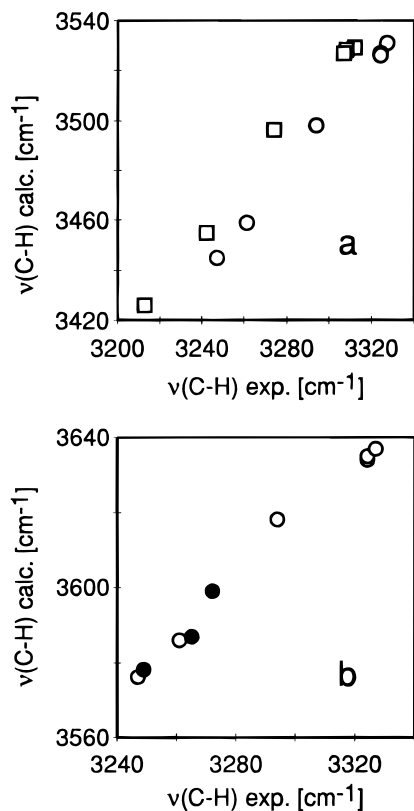


Figure 9. Correlation of the experimental C–H stretching frequencies of (a) $(\text{HCN})_n$ (squares) and $(\text{HC}_3\text{N})_n$ (circles) clusters ($n = 1-3$) with MP2(I)-derived harmonic frequencies; (b) of $(\text{HC}_3\text{N})_n$ clusters with SCF(I)-derived harmonic frequencies, the filled symbols correspond to the experimentally not yet assigned cyclic tetramer, pentamer, and hexamer, respectively.

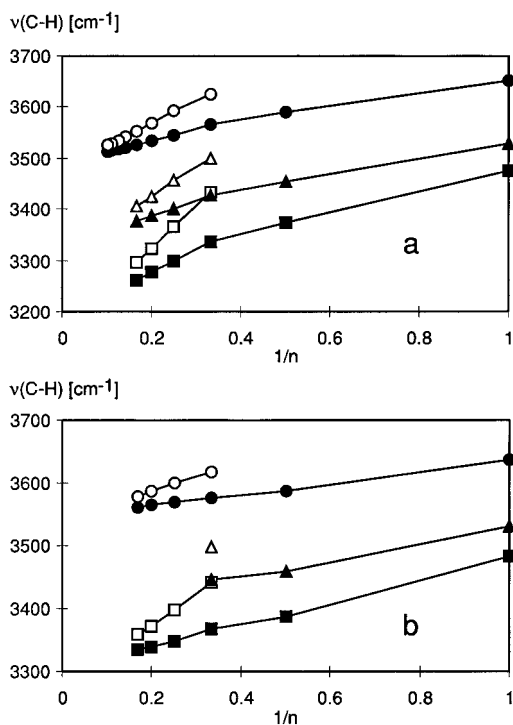


Figure 10. Plot of theoretical harmonic C–H stretching frequencies in linear and cyclic hydrogen cyanide (a) and cyanoacetylene (b) clusters vs $1/n$. n is the number of molecules in the cluster. Open symbols: cyclic clusters; filled symbols: linear clusters; circles: SCF; triangles: MP2; squares: B3LYP.

very interesting pinwheel structure suggested by Yang et al.³⁰ for the cyanoacetylene tetramer, or other possible arrangements,

require the use of quantum chemical methods that take account of electron correlation contributions at least at the MP2 level, preferably beyond. A minimum requirement that should be fulfilled is a reasonably accurate description of the global dimer intermolecular energy surfaces. Preliminary investigations of the two intermolecular energy surfaces are currently performed in our laboratory.

Acknowledgment. The calculations were performed on the RISC 6000/550-Cluster and on the Cluster of Digital Alpha Servers (2100 4/275) of the computer center of the University of Vienna. The author is grateful for ample supply of computer time on these installations and thanks Prof. Scoles and Prof. Knözinger for communicating results prior to publication and for discussions.

References and Notes

- (1) Maroncelli, M.; Hopkins, G. A.; Nibler, J. W.; Dyke, Th. R. *J. Chem. Phys.* **1985**, *83*, 2129.
- (2) Hopkins, G. A.; Maroncelli, M.; Nibler, J. W.; Dyke, Th. R. *Chem. Phys. Lett.* **1985**, *114*, 97.
- (3) Anex, D. S.; Davidson, E. R.; Douketis, C.; Ewing, G. E. *J. Phys. Chem.* **1988**, *92*, 2913.
- (4) Jucks, K. W.; Miller, R. E. *J. Chem. Phys.* **1988**, *88*, 2196.
- (5) Jucks, K. W.; Miller, R. E. *J. Chem. Phys.* **1988**, *88*, 6059.
- (6) Miller, R. E. *Science* **1988**, *240*, 447.
- (7) Ruoff, R. S.; Emilsson, T.; Klotz, T. D.; Chuang, C.; Gutowsky, H. S. *J. Chem. Phys.* **1988**, *89*, 138.
- (8) Meyer, H.; Kerstel, E. R. Th.; Zhuang, D.; Scoles, G. *J. Chem. Phys.* **1989**, *90*, 4623.
- (9) Kerstel, E. R. Th.; Lehmann, K. K.; Gambogi, J. E.; Yang, X.; Scoles, G. *J. Chem. Phys.* **1993**, *99*, 8559.
- (10) King, Ch. M.; Nixon, E. R. *J. Chem. Phys.* **1968**, *48*, 1685.
- (11) Pacansky, J. *J. Phys. Chem.* **1977**, *81*, 2240.
- (12) Walsh, B.; Barnes, A. J.; Suzuki, S.; Orville-Thomas, W. J. *J. Mol. Spectrosc.* **1978**, *72*, 44.
- (13) Knözinger, E.; Kollhoff, H.; Langel, W. *J. Chem. Phys.* **1986**, *85*, 4881.
- (14) Schrems, O.; Huth, M.; Kollhoff, H.; Wittenbeck, R.; Knözinger, E. *Ber. Bunsen-Ges. Phys. Chem.* **1987**, *91*, 1261.
- (15) Langel, W.; Kollhoff, H.; Knözinger, E. *J. Chem. Phys.* **1989**, *90*, 3430.
- (16) Beichert, P.; Pfeiler, D.; Knözinger, E. *Ber. Bunsen-Ges. Phys. Chem.* **1995**, *99*, 1469.
- (17) Dulmage, W. J.; Lipscomb, W. N. *Acta Crystallogr.* **1951**, *4*, 330.
- (18) Kofranek, M.; Karpfen, A.; Lischka, H. *Chem. Phys.* **1987**, *113*, 53.
- (19) Kofranek, M.; Lischka, H.; A. Karpfen, A. *Mol. Phys.* **1987**, *61*, 1519.
- (20) de Almeida, W. B.; Craw, J. S.; Hinchliffe, A. *J. Mol. Struct.* **1989**, *184*, 381.
- (21) de Almeida, W. B. *Can. J. Chem.* **1991**, *69*, 2044.
- (22) Kurnig, I. J.; Lischka, H.; Karpfen, A. *J. Chem. Phys.* **1990**, *92*, 2469.
- (23) King, B. F.; Weinhold, F. *J. Chem. Phys.* **1995**, *103*, 333.
- (24) King, B. F.; Farrar, T. C.; Weinhold, F. *J. Chem. Phys.* **1995**, *103*, 348.
- (25) Suhai, S. *Int. J. Quantum Chem.* **1994**, *52*, 395.
- (26) Karpfen, A. *Chem. Phys.* **1983**, *79*, 211.
- (27) Springborg, M. *Ber. Bunsen-Ges. Phys. Chem.* **1991**, *95*, 1238.
- (28) Shallcross, F. V.; Carpenter, G. B. *Acta Crystallogr.* **1958**, *11*, 490.
- (29) Kerstel, E. R. Th.; Scoles, G.; Yang, X. *J. Chem. Phys.* **1993**, *99*, 876.
- (30) Yang, X.; Kerstel, E. R. Th.; Scoles, G.; Bemish, R. J.; Miller, R. E. *J. Chem. Phys.* **1995**, *103*, 8828.
- (31) Yamada, K.; Schieder, R.; Winnewisser, G.; Mantz, A. W. Z. *Naturforsch.* **1980**, *35A*, 690.
- (32) Botschwina, P.; Horn, M.; Seeger, S.; Flügge, J. *Mol. Phys.* **1993**, *78*, 191.
- (33) Turrell, G. C.; Jones, W. D.; Maki, A. *J. Chem. Phys.* **1957**, *26*, 1544.
- (34) Uyemura, M.; Maeda, S. *Bull. Chem. Soc. Jpn.* **1974**, *47*, 2930.
- (35) Mallinson, P. D.; Fayt, A. *Mol. Phys.* **1976**, *32*, 473.
- (36) Yamada, K. M. T.; Bürger, H. Z. *Naturforsch.* **1986**, *41A*, 1021.
- (37) Nolin, C.; Weber, J.; Savoie, R. J. *Raman Spectrosc.* **1976**, *5*, 21.
- (38) Aoki, K.; Kakudate, Y.; Yoshida, M.; Usuba, S.; Fujiwara, S. *J. Chem. Phys.* **1989**, *91*, 2814.
- (39) Defrees, D. J.; McLean, A. D. *Chem. Phys. Lett.* **1989**, *158*, 540.
- (40) Hu, Ch.; Schaefer, III, H. F. *J. Phys. Chem.* **1993**, *97*, 10681.

- (41) Francisco, J. S.; Richardson, S. L. *J. Chem. Phys.* **1994**, *101*, 7707.
(42) Tostes, J. G. R.; Taft, C. A.; Ramos, M. N. *J. Phys. Chem.* **1987**, *91*, 3157.
(43) Taft, C. A.; Azevedo, J. C.; Tostes, J. G. R.; Lester, W. A., Jr. *J. Mol. Struct. (THEOCHEM)* **1988**, *168*, 169.
(44) Gaussian 94, Revision A.1, Frisch, M. J.; Trucks, G. W.; Schlegel, H. B.; Gill, P. M. W.; Johnson, B. G.; Robb, M. A.; Cheeseman, J. R.; Keith, T. A.; Petersson, G. A.; Montgomery, J. A.; Raghavachari, K.; Al-Laham, M. A.; Zakrzewski, V. G.; Ortiz, J. V.; Foresman, J. B.; Cioslowski, J.; Stefanov, B. B.; Nanayakkara, A.; Challacombe, M.; Peng, C. Y.; Ayala, P. Y.; Chen, W.; Wong, M. W.; Andres, J. L.; Replogle, E. S.; Gomperts, R.; Martin, R. L.; Fox, D. J.; Binkley, J. S.; Defrees, D. J.; Baker, J.; Stewart, J. J. P.; Head-Gordon, M.; Gonzalez, C.; Pople, J. A. Gaussian, Inc., Pittsburgh, PA, 1995.
(45) Møller, C.; Plesset, M. S. *Phys. Rev.* **1934**, *46*, 618.
(46) Becke, A. D. *Phys. Rev.* **1988**, *A38*, 3098.
(47) Lee, C.; Yang, W.; Parr, R. G. *Phys. Rev.* **1988**, *B37*, 785.
(48) Mielich, B.; Savin, A.; Stoll, H.; Preuss, H. *Chem. Phys. Lett.* **1989**, *157*, 200.
(49) Becke, A. D. *J. Chem. Phys.* **1993**, *98*, 5648.
(50) Hehre, W. J.; Ditchfield, R.; Pople, J. A. *J. Chem. Phys.* **1972**, *56*, 2257.
(51) Frisch, M. J.; Pople, J. A.; Binkley, J. S. *J. Chem. Phys.* **1984**, *80*, 3265.
(52) Huzinaga, S. *J. Chem. Phys.* **1965**, *42*, 1293.
(53) Huzinaga, S. Approximate Atomic Functions I, University of Alberta, Edmonton Canada, 1971.
(54) Botschwina, P. *Chem. Phys. Lett.* **1986**, *124*, 382.
(55) Winnewisser, G.; Maki, A. G.; Johnson, D. R. *J. Mol. Spectrosc.* **1971**, *39*, 149.
(56) Buxton, L. W.; Campbell, E. J.; Flygare, W. H. *Chem. Phys. Lett.* **1981**, *56*, 399.
(57) Boys, S. F.; Bernardi, F. *Mol. Phys.* **1970**, *19*, 553.
(58) Mettee, H. D. *J. Phys. Chem.* **1973**, *77*, 1762.
(59) Karpfen, A.; Ladik, J.; Russegger, P.; Schuster, P.; Suhai, S. *Theor. Chim. Acta (Berlin)* **1974**, *34*, 115.
(60) Karpfen A.; Yanovitskii, O. *J. Mol. Struct. (THEOCHEM)* **1994**, *314*, 211.
(61) Bendtsen, J.; Edwards, H. G. M. *J. Raman Spectrosc.* **1974**, *2*, 407.
(62) Friedrich, H. B.; Krause, P. F. *J. Chem. Phys.* **1973**, *59*, 4942.
(63) Smith, A. M.; Klemperer, W.; Lehmann, K. K. *J. Chem. Phys.* **1991**, *94*, 5040.
(64) Karpfen A.; Yanovitskii, O. *J. Mol. Struct. (THEOCHEM)* **1994**, *307*, 81.
(65) Sim, F.; St.-Amant, A.; Papai, I.; Salahub, D. R. *J. Am. Chem. Soc.* **1992**, *114*, 431.
(66) Stanton, R. V.; Merz, K. M., jr. *J. Chem. Phys.* **1994**, *101*, 6658.
(67) Latajka, Z.; Bouteiller, Y. *J. Chem. Phys.* **1994**, *101*, 9793.
(68) Zhang, Q.; Bell, R.; Truong, T. N. *J. Phys. Chem.* **1995**, *99*, 592.
(69) Latajka, Z.; Bouteiller, Y.; Scheiner, S. *Chem. Phys. Lett.* **1995**, *234*, 159.
(70) Xantheas, S. S. *J. Chem. Phys.* **1995**, *102*, 4505.
(71) Del Bene, J. E.; Person, W. B.; Szczepaniak, K. *J. Phys. Chem.* **1995**, *99*, 10705.
(72) Novoa, J. J.; Sosa, C. *J. Phys. Chem.* **1995**, *99*, 15837.

JP960599I